Effect of Spinning Conditions on the Mechanical Properties of Polyacrylonitrile Fibers Modified with Carbon Nanotubes

T. Mikolajczyk,[1,2] G. Szparaga,[1,2] M. Bogun,[1,2] A. Fraczek-Szczypta,[1,2] S. Blazewicz[1,2]

[1]*Department of Man-Made Fibers, Faculty of Textile Engineering and Marketing, Technical University, Lodz, ul. Zeromskiego 116, 90-926 Lodz, Poland*
[2]*Department of Biomaterials, Faculty of Material Science and Ceramics, AGH University of Science and Technology, al. Mickiewicza 30, 30-059 Krakow, Poland*

Received 23 October 2008; accepted 7 September 2009
DOI 10.1002/app.31414
Published online 4 November 2009 in Wiley InterScience (www.interscience.wiley.com).

ABSTRACT: Carbon nanotubes (CNTs) were used to modify polyacrylonitrile (PAN) polymer. The PAN/CNT composite fibers were spun from dimethylformamide solutions containing different types of CNTs. The effect of nanotube addition to the fiber precursor on the resulting mechanical properties is discussed. In this study, we examined the relationship of the rheological properties of PAN spinning solutions containing various types of CNTs and the tensile strength of the resulting PAN fibers. The presence of CNTs in the PAN spinning solution enhanced its deformability during the drawing stage. This effect resulted in a higher tensile strength in the fibers containing nanotubes, as compared to the pure fibers. The use of a three-stage drawing process resulted in a significant increase in the tensile strength of PAN fibers modified with multiwalled nanotubes. © 2009 Wiley Periodicals, Inc. J Appl Polym Sci 115: 3628–3635, 2010

Key words: fibers; mechanical properties; nanocomposites; rheology

INTRODUCTION

Carbon nanotubes (CNTs) are characterized by a number of unique physical and mechanical properties that are different from other forms of nanomaterials. At a high strength and Young's modulus, they show considerable flexibility and deformability in terms of twisting and bending, even at large angles. Such deformation begins with nanotube flattening without disturbance of the hexagonal lattice, which makes it possible for the nanotube to return to its initial state. Single-walled nanotubes (SWNTs) can be stretched up to 40%. Multiwalled nanotubes (MWNTs) are more effective in transmitting compressive rather than tensile stresses because of the slip of the cylindrical surfaces of graphene layers.[1–3]

At present, CNTs are being studied extensively for a variety of technical and medical applications.[4] Significant challenges are related to the development of nanocomposites consisting of polymeric matrices and CNTs. Because of their interesting physical and mechanical properties, such materials are being considered as modifying nanocomponents for various polymers in composites technology.[5–8] Among nanocomposites, polyacrylonitrile (PAN)-based composite fibers containing nanotubes seem to be particularly interesting.[9,10] The possibility to obtain carbon fibers with new engineered parameters is due not only to the modification of such precursor fibers but also to the addition of various nanocomponents, including CNTs.[11–17] An important factor affecting the resulting properties of composite fibers is a good dispersion of CNTs within a polymer precursor. A high specific surface energy makes CNTs have a tendency to form agglomerates, which may create defects inside the composite matrix.[18] The problem of the mechanical properties of a PAN fiber precursor containing CNTs is not still well solved. It was found that the PAN macromolecular orientation increases with increasing CNT orientation in the polymer, and their presence in the polymer results in a higher crystallite size in the polymer. Limited property improvement in polymer/CNT composites was observed in the presence of chaotically oriented CNTs.[10,17,19] Our previous studies have shown that different ceramic and metallic nanoparticles influence the rheological parameters of the spinning solution, the mechanism of solidification of the PAN fiber, and the deformation process during the

Correspondence to: S. Blazewicz (blazew@uci.agh.edu.pl).
Contract grant sponsor: Polish Ministry of Science and Higher Education; contract grant number: 3763/T02/2006/31.

TABLE I
Characteristics of the Nanotubes Used in the Experiments

Nanotube type	Length (nm)	Diameter (nm)	Specific surface area (m^2/g)	Producer
Chemically modified MWNTs	300–2000	5–20	20	Nanocraft (Renton, WA)
SWNTs	30–50	2–3	220	Nanocraft
MWNTs short	1000–2000	10–30	40–600	Nanostructured and Amorphous Materials, Inc. (Houston, TX)
MWNTs long	10,000–30,000	10–20	200–350	Nanostructured and Amorphous Materials, Inc.

drawing stage.[20–22] The rheological properties of the spinning solution may influence the stability of the formation process, and the possibility of the occurrence of capillary disintegration or brittle (cohesive) failure. These properties also affect the rate distributions of the liquid flow through the spinneret ducts, the relaxation processes outside the spinneret zone, and the longitudinal rate gradient along the formation pathway, which influence the structural orientation of fiber elements.

The objective of this study was to determine the influence of various types of CNTs on the rheological properties of the spinning solutions, the deformability at the drawing stage, and the resulting tensile strength of the nanocomposite PAN fibers. It is well known that the mechanical properties of PAN-based carbon fibers depend on the strength of the precursor fibers. These properties are strongly connected with the degree of structural ordering of the fibers during deformation processes.

Both the quantity and type of nanoadditive used influence on the interactions between polymer macromolecules, the solvent, and a nanoparticle. In this study, these problems were analyzed for various types of nanotubes (SWNTs and MWNTs of different lengths and MWNTs after surface functionalization).

The aim of the study was to manufacture PAN fibers as precursors for carbon fibers with diameters similar to that of microfibers. To obtain a good mechanical strength of the precursor fibers, the application of a high total deformation at the production stage was required.

In the process of PAN fiber manufacturing, it is advantageous to use a multistage drawing process in media with increasing temperature and with an appropriate distribution of deformations at the individual stages. It has been found[23] that the properties of precursor fibers are determined by the total draw ratio and also by an appropriate drawing distribution. This means that successive stages of the drawing process should be carried out with a deformation between 0.7 and 0.9% of its total value. At the last stage, the value of the deformation should be close to the maximum value achievable for given conditions. This procedure protects against the effect of the overstretching of precursor fibers, as identified in our previous study.[24] This effect may have an adverse impact on the strength properties of carbon fibers. Our method of the drawing process allows one to use potential capabilities of the material. This procedure also ensures the proper determination of the effect of the presence of various types of CNTs in the material.

EXPERIMENTAL

The spinning solution was prepared from a PAN polymer with an intrinsic viscosity of 1.46 [assayed in dimethylformamide (DMF) of the polymer at a temperature of 20°C] produced by the Zoltek Co. (Wroclaw, Poland).

The number-average molecular weight (M_n) and weight-average molecular weight (M_n) assessed by gel permeation chromatography with an *N,N*-dimethylacetamide solvent containing 0.5% lithium chloride were $M_w = 249{,}930$ and $M_n = 92577$, and the polymolecularity index was 2.7.

Four types of nanotubes were used in this study. Their characteristics are displayed in Table I.

The rheological properties of the spinning solutions were determined with a rotational rheometer (Rheotest RV) (Rheotest Messgeräte Medingen GmbH, Ottendorf-Okrilla, Germany) with an H cylinder. Measurements were carried out in ranges of the shear rate from 0.3 to 80 s^{-1} and the shear stress from 12 to1800 N/m^2 at 20°C.

The mechanical properties of pure single fibers and composite fibers were examined with a universal testing machine (Zwick 1435, Ulm, Germany) equipped with the testXpert version 8.1 program according to the standard procedure ISO 11566. A single fiber glued onto the paper frame, which had a constant grip span of 25 mm, was subjected to a uniaxial tensile force at a constant crosshead speed of 2 mm/min. Longitudinal rupture strains of the samples were obtained from the traverse displacement in tensile loading. The tensile strength was determined from the values of rupture force and the fiber cross-sectional area. This last parameter was determined with a scanning electron microscope (JEOL JSM-5200LV) by the low-pressure technique with a backscattered electron detector (at pressures of

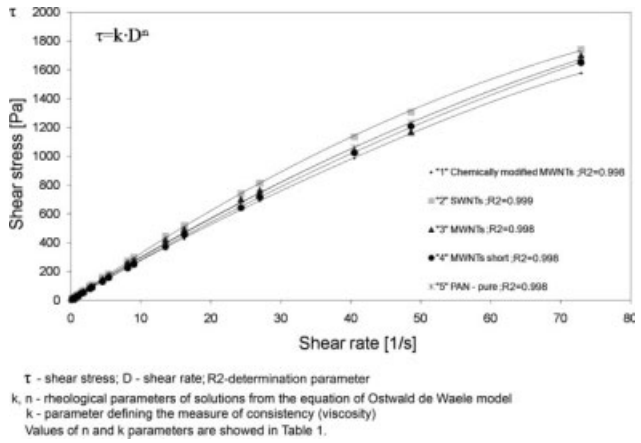

Figure 1 Relationship between the shear stress and shear rate for 23.5% PAN solutions containing 1% nanotubes.

6–270 Pa). Observations were made at an accelerating voltage of 25 kV and a magnification of 5000×. Images were recorded with a Semafore digital system. Series of 25 single fibers for each type of examined sample were tested, and the values of the tensile strength, Young's modulus, and maximum strain to break were determined as Mean ± Standard deviation. The statistical significance between two sets of data was calculated with the Student's *t* test. Data were taken to be significant when a *p* value of 0.05 or lower was obtained.

The morphology of the nanotubes was analyzed with a scanning electron microscope (Nova Nano SEM 200, FEI, Hillsboro, OR).

Fiber formation

The fibers were formed by the wet-spinning method from a solution with the use of a large laboratory spinning machine (Lodz, Poland). We used 23.5% solutions of PAN in DMF containing 1% CNTs related to the polymer weight. The spinning solutions were prepared in the following way: a homogeneous suspension of CNTs in DMF was made followed by polymer addition. The process of preparation of a nanotube suspension consisted of the homogenization of a mixture of nanotubes in DMF by means of an ultrasonic homogenizer (Bandelin Sonoplus HD 2200, Bandelin Electronic, Berlin, Germany). The process was conducted at room temperature for 30 min. The polymer was added to the prepared suspension and was then mixed (Celma-Poland, speed = 582 rpm, temperature = 55°C) until a homogeneous solution was obtained.

Fibers were spun with a 500-hole spinneret with a hole diameter of 0.08 mm.

The solidification of fibers was conducted in water baths with 60% of DMF at room temperature at an as-spun draw ratio of +75%. The as-spun draw ratio is defined as the ratio of the linear speed of the solidified fiber to the average linear speed of the stream of the spinning solution in the spinning nozzle channel.

Total deformation denotes the ratio of the speed of a fiber bundle after a technological process to the average flow speed of the spinning liquid in the channel of the spinning nozzle. Total deformation includes the as-spun draw ratio and the amount of drawing in the individual stages of the process. Deformation during drawing relates to the quantity of deformation during that process. Maximum deformation indicates the deformation for which, at a given drawing stage, there is no tearing of elementary fibers in the bundle.

The drawing process was conducted in a two- or three-stage procedure. In the case of the two-stage drawing process, the first stage was conducted in an aqueous plasticizing bath containing 50% DMF at a temperature of 70°C and at 0.7% maximum deformation. The second stage was conducted in superheated steam at a temperature of 135°C at maximum deformation. After the drawing process, the fibers were rinsed and dried at room temperature.

In three-stage drawing, the first stage was conducted in the same way as the first variant, whereas in the second stage, a value of 0.9% of the maximum deformation was applied. After the second drawing stage, the fibers were rinsed to remove the remaining solvent and subsequently dried and drawn in superheated steam at a temperature of 165°C. This last drawing stage was conducted at maximum deformation. Such a procedure was adopted because, according to our research,[23] the strength properties of precursor fibers are determined not only by the size of the total draw ratio but also by an appropriate distribution of drawing values at each stage of a multistage process. The +75% value of the as-spun draw ratio allowed for the orientation of structural elements and CNTs in the fluid stream. This value was selected on the basis of preliminary tests.

DISCUSSION

Figure 1 gathers the flow curves of PAN solutions with different nanotubes. The upper curves correspond to the solution containing SWNTs (curve 2)

TABLE II
Rheological Parameters of PAN Solutions in DMF Containing Different Nanotubes

Type of nanotubes	*n*	*k*
Chemically modified MWNTs	0.969	28.04
SWNTs	0.952	35.65
Long MWNTs (length = 15–30 μm)	0.948	33.47
Short MWNTs (length = 1–2 μm)	0.972	28.69
Pure PAN solution	0.968	30.28

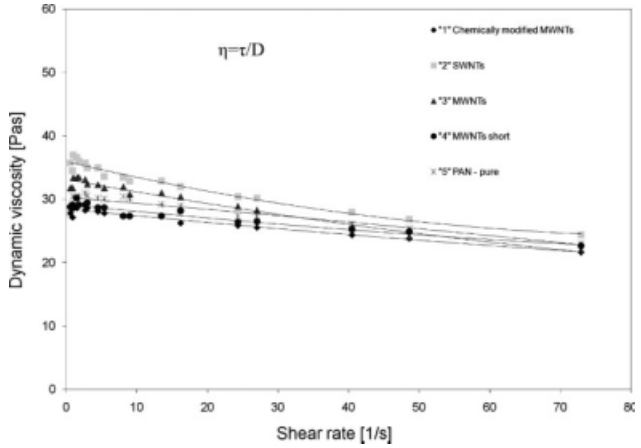

Figure 2 Relationship between the apparent dynamic viscosity (η) and shear rate for 23.5% PAN solutions containing 1% nanotubes.

and long MWNTs (curve 3). The flow curve for the pure solution (without nanotubes) is in the middle (curve 5). The character of the flow curves showed that, regardless of the type of nanoadditive used, the solutions behaved as non-Newtonian fluids, thinned with shearing without a flow limit. It can be described by the power model of Ostwald de Waele:

$$\tau = kY_x^n \tag{1}$$

where n and k are rheological parameters of the model, Y_x is the shearing rate, and τ is the shearing stress.

The rheological parameters n and k however changed (Table II). The character of the solutions containing SWNTs and long MWNTs diverged from Newtonian characteristics more significantly, which was documented by their rheological parameters. Solutions containing short MWNTs and nanotubes functionalized by acidic chemical treatment were closer to Newtonian fluids. Their flow parameter n was 0.97, which was similar to typical pure solutions. At the same time, these solutions revealed a less polymer-like character. Their rheological parameter k, which determines the consistency of solutions, was lower than that for solutions containing the SWNTs and long MWNTs. Figure 2 represents the variations in apparent absolute viscosity of the solutions as a function of shear rate. The runs were consistent with the runs shown in Figure 1. This different rheological behavior of fluids was probably related to the different structures and properties of the particular types of nanotubes. Considering their influence on the spinning solution with respect to the known explanation of shear thinning mechanism, we found the following interpretation probable: the phenomenon of shear thinning[21] was

TABLE III
Spinning Conditions and Properties of PAN Fibers Modified with Nanotubes

Sample fiber	Type of nanotube	Drawing (%)				Total deformation	Diameter (μm)	Young's modulus (GPa)	Tensile strength (MPa)	Absolute random error (MPa)	Strain to failure (%)
		R_1	R_2	R_3	R_{tot}						
SR3	Modified MWNTs	339.32	131.04	–	915.00	17.76	10.4 ± 0.31	10.3 ± 0.31	570 ± 17	8.00	12.71 ± 0.38
SR3/1	Modified MWNTs	339.32	117.94	17.03	1070.82	20.79	9.8 ± 0.29	12.1 ± 0.36	570 ± 17	8.00	8.36 ± 0.25
SR5	SWNTs	306.70	155.33	–	938.42	18.17	9.9 ± 0.30	10.3 ± 0.31	560 ± 17	8.00	11.70 ± 0.35
SR5/2	SWNTs	306.70	139.80	16.39	1092.23	21.15	9.6 ± 0.29	11.5 ± 0.34	540 ± 16	7.49	8.22 ± 0.25
SR7	Long MWNTs	314.83	168.91	–	1015.53	19.52	9.3 ± 0.28	8.6 ± 0.26	540 ± 16	7.49	11.37 ± 0.34
SR7/1	Long MWNTs	314.83	152.02	20.22	1220.87	23.47	9.0 ± 0.27	12.18 ± 0.36	620 ± 19	8.89	8.22 ± 0.25
SR9	Short MWNTs	336.70	156.42	–	1019.80	19.60	8.9 ± 0.27	10.4 ± 0.31	570 ± 17	8.00	11.87 ± 0.36
SR9/1	Short MWNTs	336.70	140.78	9.70	1118.72	21.50	8.8 ± 0.26	11.0 ± 0.33	630 ± 19	8.89	8.53 ± 0.26
SN13 (pure)	–	295.22	166.95	–	955.04	18.46	9.7 ± 0.29	7.8 ± 0.23	510 ± 15	7.02	12.84 ± 0.38
SN13/1 (pure)	–	295.22	150.25	7.22	953.24	18.56	9.2 ± 0.28	9.5 ± 0.28	530 ± 16	7.49	9.18 ± 0.27

R_1 = value of the draw ratio in the first stage of drawing; R_2 = value of the draw ratio in the second stage of drawing; R_3 = value of the draw ratio in the third stage of drawing; R_{tot} = total draw ratio.

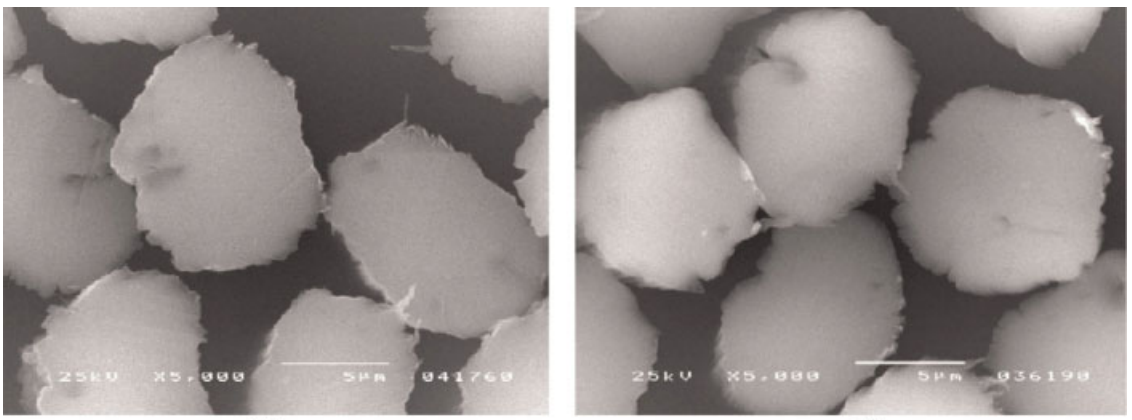

Figure 3 Cross-sectional areas of the nanocomposite fibers after (A) two-stage (SR5) and (B) three-stage (SR5/2) drawing processes.

considered a result of the orientation of dispersed polymer macromolecules and the immobilization of the continuous phase of the solvent. In an immobile fluid, the effective sizes of macromolecules with an immobilized continuous phase are significant. In case of short MWNTs, a part of this phase (solvent) may have been located inside them. On the contrary, the penetration of very long MWNTs by the solvent was more difficult. SWNTs may be closed at one or both ends, which makes it difficult or impossible for the solvent to penetrate them. Upon shearing, the polymer macromolecules began to straighten. The faster the shearing was, the larger the effect was. This led to a decrease in the internal friction of the fluid because of the smaller dimensions of macromolecules and weaker interaction between them. The presence of short MWNTs and SWNTs between macromolecules may have facilitated macromolecule slip, which led to a reduction in the internal friction of the fluid. As was already discussed in our previous articles, the presence of different types of ceramic particles in the form of nanopowders, especially montmorylonite (MMT) induces the opposite effect.[12–15] In the case of functionalized nanotubes containing chemical groups on their surface, a specific interaction with the polymer matrix may occur. The internal friction of the sheared fluid is influenced by the interactions both of the nanotubes with polymer macromolecules and of the surface with the solvent particles. Thus, the solutions containing long MWNTs behaved like highly consistent fluids and showed stronger non-Newtonian characteristics. It was also related to SWNT nanotubes. It is known that the phenomenon of shear thinning may be caused by solvation, namely, by the addition of particles to the continuous phase (the solvent) through dispergation of a polymer macromolecule or a solid particle (CNTs). A gradual wearing the solvation shell in such a system (with increasing shear rate) results from the interaction between polymer particles with the solvent and in a significant way with CNTs. As a result, the internal friction of the system decreases, depending on the type of nanotubes and their interaction with the solvent.

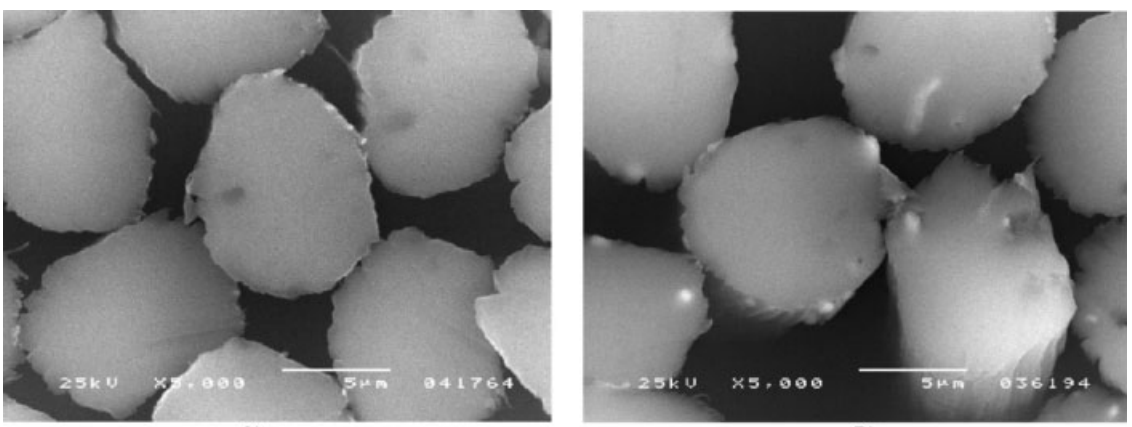

Figure 4 Cross-sectional areas of the nanocomposite fibers after (A) two-stage (SR9) and (B) three-stage (SR9/1) drawing processes.

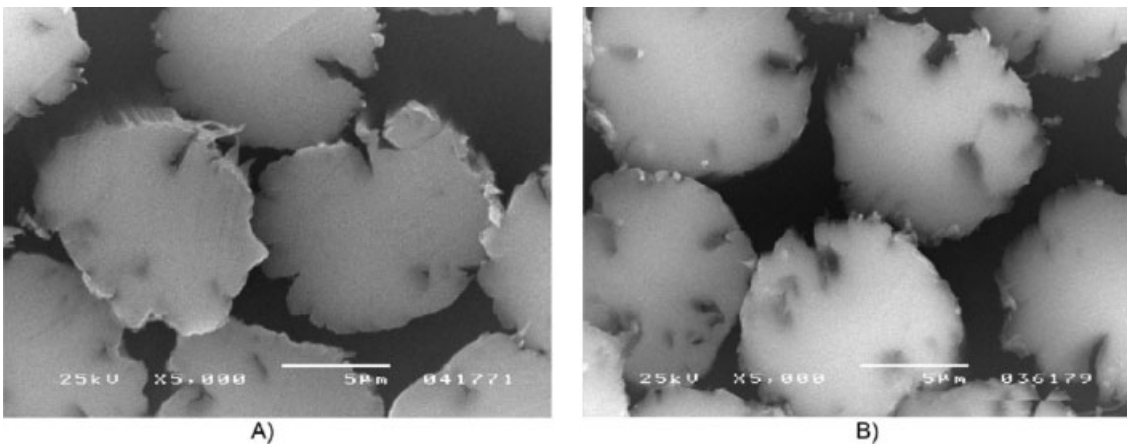

Figure 5 Cross-sectional areas of the fibers without CNTs after (A) two-stage (SR13) and (B) three-stage (SR13/1) drawing processes.

The type of nanotubes added to the spinning solution also determined the deformation processes at the drawing stage.

The two-stage drawing process (the first stage conducted at 0.7% of the deformation maximum and second one conducted at the deformation maximum) allowed us to obtain high total deformations of 17.7–19.5. This was possible due to of the application of high positive values of the as-spun draw ratio (+75%) at the solidification stage. Such values of the as-spun draw ratio enabled the deformation of a fluid polymer filament and the streamline orientation of the structural elements, which resulted from an increase in the longitudinal rate gradient. This orientation may have been decisive for the resulting structure and mechanical parameters of the nanocomposite fibers. In the drawing process of a gradually solidifying fluid, the rheological resistance is too small to decrease the longitudinal rate gradient. Under the circumstances, it is easier to orient both the macromolecules and the nanotubes in the solution. The structure formed after the solidification stage also determines deformability at the drawing stage. Under similar drawing parameters in the plasticizing bath, in the range 306–339%, the highest total deformation (>19.5) was obtained for the fibers containing short and long MWNTs. This deformation was much higher than that of the pure fibers formed under similar conditions (Table III). A similar total deformation at a level of 17.6–18.1 was obtained for the fibers containing SWNTs and functionalized nanotubes. The different contribution of particular types of nanotubes in the deformation processes may have resulted from their different shapes and sizes. The SWNTs were probably less susceptible orientation in the polymer solution along the fiber axis.

As a result of such deformation processes, a fiber diameter of less than 10 μm was obtained (except for the chemically modified nanotubes). Their tensile strength after a two-stage drawing process was 540–570 MPa. The highest strength of 570 MPa was obtained for the fibers containing short MWNTs, for which a highest total deformation of 19.6 was applied. Fibers containing SWNTs and long MWNTs had slightly lower tensile strengths of 540–560 MPa. The highest value of tensile strength for fibers containing chemically modified nanotubes (570 MPa) was obtained under their lower deformability.

The tensile strength of fibers spun from the pure solution (without nanotubes) was 510 MPa, which was consistent with their deformability at the solidification and drawing stages. This deformability was lower than that of fibers containing nanotubes.

Our previous study indicated that PAN fibers containing various ceramic nanoadditives (SiO_2 and MMT) demonstrated a significantly lower deformability, and their tensile strength properties were much lower compared to the fibers without nanoadditives.[15]

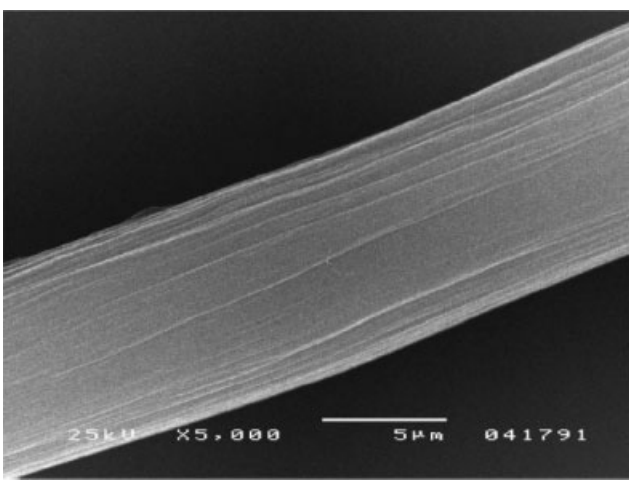

Figure 6 Surface of the nanocomposite fibers (SR9).

Further improvement in the strength of the nanocomposite fibers were obtained in a three-stage drawing process. It is known[23] that the fiber strength depends not only on the degree of total deformation but also on the proper distribution of the drawing values between the subsequent stages of the process. The process was conducted at 0.7% of maximum deformation in the first stage and 0.9% in the second stage. In the third stage, the applied deformation coresponded to the maximum deformation possible to be obtained for fibers with a given type of nanotubes. Such a drawing process made it possible to obtain a very high total deformation. Depending on the nanotubes used, it was 21–23.5. As in the two-stage drawing, the highest total deformation was obtained for short and long MWNTs. This resulted in an increase in the fiber tensile strength by 60 and 80 MPa, respectively. For the other types of nanotubes, such a phenomenon was not observed, although fibers containing them were also formed at a high total deformation of about 21. On the other hand, fibers without nanotubes formed under similar conditions revealed a much lower tensile strength (Table III). After the two-stage drawing process, the tensile strength was lower by 60 MPa, whereas after the three-stage process, the strength decreased by 100 MPa, as compared to fibers with short MWNTs. An important finding of these experiments is that the main cause of a better deformability and higher tensile strength of the nanocomposite fibers was the presence of CNTs in the fiber matrix. Their presence also decreased the internal friction of the system. Their impact may be compared to the role of a plasticizer facilitating macromolecule slip in the drawing process.

The obtained differences between the mean values of the tensile strengths for all of the analyzed samples obtained in the three-stage drawing process (gathered in Table III) were statistically significant ($p < 0.05$). For only one variant (SR5/2–SN13/1) were the differences not statistically significant.

The differences in the structure of the nanotubes (SWNTs or MWNTs) may have also been the reason for the different tensile strength properties of particular types of nanocomposite fibers. The structure of the nanotubes may have influenced the macroscopic structure, total volume of pores, type of porosity, and supramolecular structure of the fibers. This last feature may have resulted from the different susceptibilities of the nanotubes to orientation along the fiber axis.

Scanning electron microscopy images of the cross sections of the pure fibers and fibers containing various types of nanotubes are shown in Figures 3–5. Figures 3(A), 4(A), and 5(A) show the fibers obtained in the two-stage drawing process, whereas Figures 3(B), 4(B), and 5(B) show the fibers manufactured in the three-stage process. The shape of the cross section of these fibers was almost circular, with small irregularities at the edge line. Pure fibers (without nanotubes) were characterized by the presence of radially distributed pores, visible on the cross-sectional area in the form of darkened areas (Fig. 5). Some of these pores were completely open or were bottlelike, closed at the end. Such pores appeared in the fibers obtained both in the two-stage and three-stage stretching processes. This type of microporous structure was found in most of the fibers in the bundle. Nanocomposite fibers, both after the two-stage drawing process [Figs. 3(A) and 4(A)] and after the three-stage process [Figs. 3(B) and 4(B)], had a very uniform cross section. The observed differences in the macroscopic structure of the two types of fibers confirmed the effect, which we identified earlier,[22] of various types of nanoadditives on the slow of the mass exchange processes at the solidification stage. This type of structure of nanocomposite fibers is typical for solidification processes by a diffusion mechanism. The surface of the fibers formed from the solution (Fig. 6) for SR9 fibers was characterized by the presence of scratches and cracks. A detailed comparative analysis of the porous and supramolecular structure of PAN fibers modified with various types of CNTs with respect to their tensile strength properties will be the subject of another publication.

CONCLUSIONS

1. The addition of CNTs to a PAN spinning solution in DMF caused an increase in its consistency. The fluid became more non-Newtonian in character, being thinned all the time by shearing without a flow limit. The rheological parameters n and k depended on the type of nanotubes and their various interactions with the solvent and polymer macromolecules.
2. The presence of CNTs in the PAN fiber matrix enhanced its deformability at the drawing stage. This effect resulted in a higher tensile strength in the fibers containing nanotubes, as compared to the pure fibers, to a degree depending on the type of nanotubes (SWNTs or MWNTs).
3. The use of a third drawing stage resulted in a significant increase in the tensile strength in the PAN fibers modified with MWNTs.

References

1. Ajayan, P. M.; Schadler, L. S.; Giannaris, C. Adv Mater 2002, 12, 750.

2. Jortner, J. C.; Rao, N. R. Pure Appl Chem 2002, 74, 1491.
3. Dresselhaus, M. S.; Dresselhaus, G. Carbon Nanotubes: Preparation and Properties; CRC: New York, 1996.
4. Rotkin, S. V.; Subramoney, S. Applied Physics of Carbon Nanotubes; Springer-Verlag: Berlin, 2005.
5. Lau, K. T. Carbon 2002, 40, 1605.
6. Andrews, R.; Jacques, D.; Minot, M.; Rantell, T. Macromol Mater Eng 2002, 287, 395.
7. Gojny, F. H.; Nastalczyk, J.; Roslaniec, Z.; Schulte, K. Chem Phys Lett 2003, 370, 820.
8. Owens, F. J. Mater Lett 2005, 59, 3720.
9. Chae, H. G.; Sreekumer, T. V.; Uchida, T.; Kumar, S. Polymer 2005, 46, 10925.
10. Sreekumar, T. V.; Liu, T.; Min, B. G.; Guo, H.; Kumar, S.; Hauge, R. H.; Smalley, R. E. Adv Mater 2004, 16, 58.
11. Mikolajczyk, T.; Bogun, M.; Blazewicz, M.; Piekarczyk, I. J Appl Polym Sci 2006, 100, 2881.
12. Mikolajczyk, T.; Bogun, M.; Kowalczyk, A. Fibres Text East Eur 2005, 13(3), 30.
13. Bogun, M.; Mikolajczyk, T.; Kurzak, A.; Blazewicz, M.; Rajzer, I. Fibres Text East Eur 2006, 14(2),13.
14. Bogun, M.; Mikolajczyk, T. Fibres Text East Eur 2006, 14(3), 19.
15. Mikolajczyk, T.; Bogun, M.; Rabiej, S. J Appl Polym Sci 2007, 105, 2346.
16. Mikolajczyk, T.; Rabiej, S.; Bogun, M. J Appl Polym Sci 2006, 101, 760.
17. Chae, H. G.; Sreekumar, T. V.; Uchida, T.; Kumar, S. Polymer 2005, 46, 10925.
18. Fornes, T. D.; Baur, J. W.; Sabba, Y.; Thomas, E. L. Polymer 2006, 47, 1704.
19. Xie, X. L.; Mai, Y. W.; Zhou, X. P. Mater Sci Eng R 2005, 49, 89.
20. Mikolajczyk, T.; Janowska, G.; Wojcik, M.; Bogun, M.; Kurzak, A. J Appl Polym Sci 2008, 109, 2513.
21. Mikolajczyk, T.; Bogun, M.; Kurzak, A.; Wojcik, M.; Nowicka, K. Fibres Text East Eur 2007, 15, 19.
22. Mikolajczyk, T.; Szparaga, G.; Janowska, G. Polym Adv Technol, to appear.
23. Mikolajczyk, T.; Olejnik, M. Fibres Text East Eur 2009, 17(1), 20.
24. Mikolajczyk, T. Fibres Text East Eur 1997, 5, 42.